Sensor systems

Hardness Discrimination Using Piezoelectric-Based Biomimetic Tactile Sensor and Machine Learning

Hussein Bassal[1], Yahya Abbass[1], Christian Gianoglio[1*], and Maurizio Valle[1**]

Department of Electrical, Electronic, Telecommunications Engineering, and Naval Architecture (DITEN), University of Genoa, 16145 Genova, Italy

[*] *Associate Member, IEEE*

[**] *Senior Member, IEEE*

Manuscript received 30 April 2024; revised 24 June 2024 and 5 July 2024; accepted 17 July 2024. Date of publication 19 July 2024; date of current version 30 July 2024.

Abstract—In this letter, we present a tactile sensing system based on piezoelectric sensors, embedded electronics, and a machine learning (ML)-based approach for hardness discrimination. Various statistical features were extracted and evaluated through machine learning algorithms including support vector machines (SVM), single-layer feed-forward neural networks, and k-nearest neighbor (KNN). Five hardness objects were examined by performing indentation experiments using a Cartesian robot equipped with the sensing system while varying the indentation speed and load. Results showed that the SVM classifier trained on features ranked using principal component analysis (PCA) achieves a discrimination accuracy of 96% while utilizing a single sensor. Furthermore, results demonstrated that fixing the indentation speed and load increases the discrimination accuracy to 100%. This study demonstrated the capability of the tactile sensing system in extracting tactile information opening up interesting perspectives for wearable sensing and soft robots.

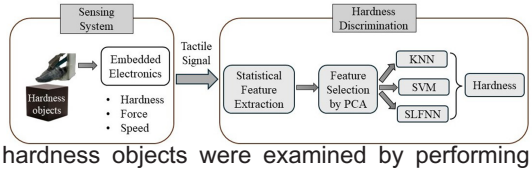

Index Terms—Sensor systems, hardness discrimination, machine learning (ML), signal processing, tactile information, tactile sensing.

I. INTRODUCTION

Humans can explore diverse objects and simultaneously infer their material properties, a challenging task for robots characterized by the lack of effective sensing systems. This lack can affect different modalities of sensation and control including touch, pressure, and proprioception [1], [2]. Until now, it remains challenging to simulate the human sense of touch as it does not reflect only the tactile response to external physical stimuli (e.g., pressure), but also the material properties (e.g., hardness) through extraction and analysis of information [3]. Hardness, as an important physical property of objects, directly impacts the grasping success of robots. It was proved that discrimination of an object's hardness increases proprioceptive, tactile discriminative, and object recognition senses along with postural control [4]. To this end, hardness perception and intelligent controls can be designed based on the development of tactile sensors [5] and machine learning (ML) techniques [6].

Tremendous sensing technologies based on intelligent tactile sensors [3] and ML techniques [6] have been developed to recognize the material's properties. Considering hardness as a key feature for efficient motor control of robotic hands [7], many tactile sensors based on various sensing mechanisms were developed and used for hardness recognition. For example, the researchers of [8] utilized an optical tactile sensor for tissue hardness discrimination. On the other hand, the researchers of [9] developed a membrane-like piezoresistive flexible tactile to discriminate six objects with different hardness. A bionic tactile sensor based on polyvinylidene fluoride (PVDF) tactile sensors was developed in [10] and used to detect the hardness of three latex samples during tapping experiments. Neural network algorithms were trained on the time-domain features of the PVDF signals and used to discriminate the hardness of the samples. The authors of [11] calculated the hardness using the load measured by a commercial tactile sensor mounted on an RH8D five-fingered robotic hand. The authors programmed the hand to grasp the object with constant speed and then employed several ML models including a support vector machine (SVM) for object recognition. Similarly, the authors of [12] combined a commercial tactile sensor array, principal component analysis (PCA), k-nearest neighbor (KNN), and SVM to recognize the hardness of fruits and vegetables. The authors mounted the sensors on a robotic gripper that manipulates the vegetables at constant force and speed, thus limiting the experimental conditions. Despite the great advancement in hardness classification, most of the works in the literature proposed complex hardness approaches. Moreover, these approaches were validated in a controlled manner, in which the gripping speed and load of the manipulator were fixed. This is important as humans use specific movement strategies to extract information about object properties during haptic exploration [13]. Moreover, the relationship between fundamentally different sensory parameters must be known to treat these parameters as relating common object or property [14]. Therefore the load and speed one employs to explore the object affects the perception of its softness since they may alter the intensity and frequency content of the vibrations it elicits in the skin [15]. Therefore, it is crucial to consider the tactile motion alongside the sliding speed and load while developing a tactile sensing system for hardness identification. Moreover, it is generally difficult for robotics to sense the material hardness using one single sensor [16]. To that aim, this

Corresponding author: Yahya Abbass (e-mail: yahya.abbass@unige.it).
Associate Editor: Sheng-Shian Li.
Digital Object Identifier 10.1109/LSENS.2024.3431430

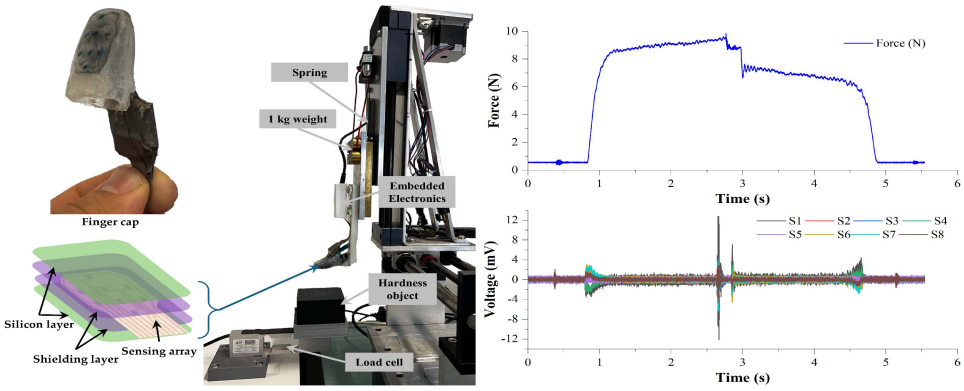

Fig. 1. Left: Experimental setup used to collect the hardness dataset. Indentation actions were applied by the mean of a Cartesian robot on a 3-D object with different hardness. Right: Response of the Load cell (Top) and eight PVDF sensors to indentation.

article attempts to develop a tactile sensing system that is composed of a PVDF-based biomimetic finger cap, embedded electronics, and ML algorithms for hardness discrimination in wearable and soft robots. In this study, we demonstrate the system's capability of sensing the relative hardness of objects through a simple operation mechanism. Combined with feature extraction and ML, the sensing system can perceive with high accuracy the object's hardness considering the change in the indentation speed and load whil32-channelg a single sensor. To the best of the authors' knowledge, this is the first hardness discrimination approach that considers the indentation speed and load as key parameters and uses a single sensor.

II. MATERIALS AND METHODS

A. Tactile Sensing System

The flexible sensor array is based on poly(vinylidene fluoride trifluoro-ethylene) piezoelectric polymer sensors fabricated following the procedure described in [17]. The sensor array is composed of eight sensors screen-printed on a transparent and flexible (175 μm thick) DIN A4 plastic foil (MelinexST 725) substrate. The sensing array was shielded using conductive tapes following the procedure presented in [18] then sandwiched between two silicon caps forming a sensorized finger cap (see Fig. 1-Top). An embedded electronics was configured to acquire and process tactile data from the eight sensors at a sampling rate of 2 kHz covering the full bandwidth of the PVDF sensor ($\leq$0.5 Hz $-$1 kHz). It is based on a 32 channel analog-to-digital converter (DDC232) and a low-power ARM cortex-M0 microcontroller [18].

B. Experimental Setup

This letter aims to assess the ability of the tactile sensing system to capture hardness features in indentation experiments. To that aim, the 3-D-printed objects presented in [19] were utilized in this study. Five cubic objects ($7 \times 7 \times 4$ cm^3) were 3-D printed with five different filling percentages (3%, 5%, 7%, 10%, and 12%) using thermoplastic polyurethane. Unlike the experiments in [19], in this study, we considered the indentation speed and load. For that reason, a three-axis Cartesian robot was used to perform a series of indentation actions on the 3D-printed objects through the z-axis. The z-axis is driven by a stepper motor and is controlled by modulating the z-coordinates and indentation speed. To modulate the load on the surface of the skin patch gradually, a 1 kg weight was mounted on the z-axis and hung to spring as shown in Fig. 1. The finger cap and embedded electronics were mounted on a 3D finger-shaped support and then fixed to the z-axis of the Cartesian robot (see Fig. 1). To measure the load applied through the z-axis on the objects, the 3-D objects were placed on a load cell (Tedea Huntleih, Model 1042), which is mounted in line with the z-axis.

C. Data Collection and Preprocessing

In this study, indentation experiments were planned to perform human-like contact to perceive the hardness of the objects however while controlling the speed and load. To that aim, different mechanical inputs were applied by programming the Cartesian to press the 3-D objects using the sensorized finger while measuring continuously the electrical response of the PVDF sensors and the reference load cell. The indentation procedure consisted of the following steps: indentation (initial load: 8 N), increasing the load to a target value [target load (TL)], decreasing the load to the initial load, and then releasing the finger gradually. The aforementioned sequence was repeated for four TL {8.5, 9.5, 10.5, 11} N at three Indentation Speeds (IS) {2.4, 5.6, and 7.2} (mm/s). Then, repeated for each 3D-printed object, thus generating a dataset composed of 60 combinations of objects, TL, and IS. Finally, each combination was repeated for 10 trials. The dataset can be formulated as $\mathcal{D} = \{(X_i, y_i),\ X_i \in \mathbb{R}^{N_C \times N_S},\ y_i \in \{five\ hardnesses\};\ i = 1, \ldots, 600\}$, where X_i is a 2-D tensor with $N_C = 8$ representing the number of channels (i.e., the sensors) and N_S the number of samples that depends on the TL and IS. Fig. 1 (top-right) shows an example of the indentation sequence at an IS of 5.6 mm/s and a TL of 10.5 N, while Fig. 1 (bottom-right) the corresponding eight PVDF sensors outputs. The rapid decrease in the force around 3 s is a spontaneous event due to the spring used to increase the load gradually.

To reduce the complexity of the proposed approaches, we consider selecting only the most active sensors. For that reason, the energy along each sensor was computed for each $X_i \in \mathcal{D}$ to determine the most active sensor. As a result, a new dataset $\tilde{\mathcal{D}}$ was extracted from $\mathcal{D}$, which can be formulated as $\tilde{\mathcal{D}} = \{(\tilde{X}_i, y_i),\ \tilde{X}_i \in \mathbb{R}^{1 \times N_S},\ y_i \in \{\ldots\}\}$. Inspired by the work done in [12] and [19], five features were extracted for each $\tilde{X}_i \in \tilde{\mathcal{D}}$. Specifically, the set of features $f5 = \{$Standard Deviation (STD), Skewness (SK), Kurtosis (KT), Peak-to-Peak (PP), STD of differences between adjacent samples (SD)$\}$. Consequently, each $\tilde{X}_i \in \tilde{\mathcal{D}}$ was transformed to $\tilde{X}_i^{f5} \in \tilde{\mathcal{D}}^{f5}$, where $\tilde{\mathcal{D}}^{f5} = \{(\tilde{X}_i^{f5}, y_i),\ \tilde{X}_i^{f5} \in \mathbb{R}^{1 \times 5},\ y_i \in \{\ldots\}\}$. The PCA technique [20] was then applied on $\tilde{\mathcal{D}}^{f5}$ to determine the best representative feature, thus reducing the dataset dimensions. Fig. 2 shows the PCA biplot computed on $\tilde{\mathcal{D}}^{f5}$ to insight the best

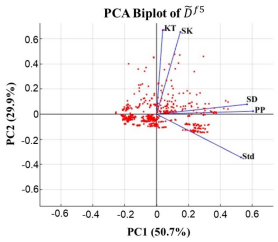

Fig. 2. PCA Biplot of the extracted features in $\tilde{\mathcal{D}}^{f5}$. Blue lines represent the feature vectors indicating the relevance of each feature.

combination of features. The length of the feature vectors and the angles between the lines reflect the relevance and the correlation of the represented features [21]. Hence, features were ranked by multiplying the biplot coordinate values of each feature by the corresponding component explainability, ranking the extracted features as follows $\{STD \rightarrow PP \rightarrow SD \rightarrow SK \rightarrow KT\}$. To study the impact of the number of features (i.e., computation complexity), three subsets of features, $f2$, $f3$, and $f4$, were selected from the list of the ranked features. The list subsets $f2$, $f3$, and $f4$ represent the most two, three, and four relevant features, respectively. As a result, from each $\tilde{X}_i^{f5} \in \tilde{\mathcal{D}}^{f5}$, $\tilde{X}_i^{f2}$, $\tilde{X}_i^{f3}$, and $\tilde{X}_i^{f4}$ were extracted, with f2 = {STD, PP}, f3 = {STD, PP, SD}, and f4 = {STD, PP, SD, SK}. Hence, three more datasets were generated, i.e., $\tilde{\mathcal{D}}^{fj} = \{(\tilde{X}_i^{fj}, y_i),\ \tilde{X}_i^{fj} \in \mathbb{R}^{1\times j},\ y_i \in \{\ldots\}\}$ with $j = \{2, 3, 4\}$ indexing the subset of features. The four datasets $\tilde{\mathcal{D}}^{f2}$, $\tilde{\mathcal{D}}^{f3}$, $\tilde{\mathcal{D}}^{f4}$, and $\tilde{\mathcal{D}}^{f5}$ were used to train and test the ML algorithms described in the next section.

To demonstrate the impact of IS and TL on the discrimination capability of the developed system, each of datasets $\tilde{\mathcal{D}}^{f2}$, and $\tilde{\mathcal{D}}^{f5}$ were divided into 12 subdatasets representing the combination between the IS and TL. As a result, each $\tilde{X}_i^{f2} \in \tilde{\mathcal{D}}^{f2}$ and $\tilde{X}_i^{f5} \in \tilde{\mathcal{D}}^{f5}$, was transformed into $\tilde{X}_{ic}^{f2} \in \tilde{\mathcal{D}}_c^{f2}$ and $\tilde{X}_{ic}^{f5} \in \tilde{\mathcal{D}}_c^{f5}$ respectively, where $\tilde{\mathcal{D}}_c^{f2} = \{(\tilde{X}_{ic}^{f2}, y_i),\ \tilde{X}_{ic}^{f2} \in \mathbb{R}^{1\times k},\ y_i \in \{\ldots\};\ i = 1, \ldots, 50\}$, $\tilde{\mathcal{D}}_c^{f5} = \{(\tilde{X}_{ic}^{f5}, y_i), \tilde{X}_{ic}^{f5} \in \mathbb{R}^{1\times c},\ y_i \in \{\ldots\};\ i = 1, \ldots, 50\}$ and c representing the IS and TL combinations $\{[TL = 8.5,\ IS = 2.4], \ldots, [TL = 11,\ IS = 7.2]\}$. The 12 datasets $\tilde{\mathcal{D}}_c^{f2}$ $(c = \{1, \ldots, 12\})$ were also used to train and test the ML algorithms.

D. Hardness Discrimination Algorithms

Three discrimination algorithms were evaluated as they met with significant success in numerous real-world discrimination tasks [12], [19], [22]. The algorithms are a SVM, a single-layer feedforward neural network (SLFNN), and a KNN.

1) Support Vector Machine: The SVM classifier is a supervised ML algorithm that computes the hyperplane that maximizes the margin to the nearest samples of the classes. The Gaussian kernel was employed to project the data into a new space.

2) Single-Layer Feedforward Neural Network: An SLFNN is a fully connected network with only one single hidden layer trained through the gradient-descent backpropagation technique. The rectified linear unit (ReLU) function was used as an activation function for the hidden neurons and an output layer comprised five neurons to classify the five textures.

3) K-Nearest Neighbor: The class of a test sample is determined by taking the majority vote of class labels among the K-closest training samples. The Euclidean distance was employed.

All the algorithms were trained and tested on fivefolds using a stratified cross-validation technique applied to each dataset, where the stratification balances the number of samples per class in each fold. Then, four out of five folds, in rotation, were used for training and the remaining fold was used for the testing. The training set was subsequently divided into training (80%) and validation (20%) sets. The validation set was employed to determine the optimal configuration of hyperparameters. Specifically, for the SVM, this included the standard deviation for the Gaussian kernel and the l2-regularizer parameter; for the SLFNN, it encompassed the number of neurons in the hidden layer and the l2-regularizer parameter; while for the KNN, optimization involved the K parameter.

TABLE 1. Average Discrimination Accuracy (Acc) and Standard Deviation (SD) of the ML Algorithms Over fivefolds on the Four Datasets

Dataset	Acc ± SD (%)		
	SVM	SLFNN	KNN
$\tilde{\mathcal{D}}^{f2}$	82.2 ± 3	77.3 ± 6	80.7 ± 4
$\tilde{\mathcal{D}}^{f3}$	89.3 ± 2	86.3 ± 9	88.3 ± 1
$\tilde{\mathcal{D}}^{f4}$	91.8 ± 4	91.8 ± 8	92.3 ± 2
$\tilde{\mathcal{D}}^{f5}$	96.5 ± 2	96.2 ± 6	94.6 ± 1

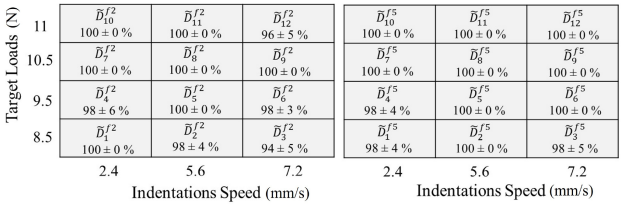

Fig. 3. Average discrimination accuracy of SVM algorithm when trained on datasets with fixed IS and TL.

III. RESULTS AND DISCUSSION

Table I summarizes the average discrimination accuracy for each ML algorithm over four datasets (Section II-C). The three models exhibit an increase in discrimination accuracy as a function of the number of features, thus highlighting the importance of the extracted features. In general, The three ML algorithms performed similarly over the four datasets, however, SLFNN possesses the lowest accuracy of 77.3% when trained on the smallest dataset $\tilde{\mathcal{D}}^{f2}$ (2 features out of 5). As expected, training the ML algorithm using $\tilde{\mathcal{D}}^{f2}$ results in an increase of $\gtrsim 10\%$ in the average discrimination accuracy for all the algorithms. Therefore, involving the SD features ($\tilde{\mathcal{D}}^{f3}$) in training the three algorithms results in a $\sim 10\%$ increase in the accuracy confirming the outcome of the PCA biplot. This is confirmed when adding less important features to the training dataset ($\tilde{\mathcal{D}}^{f4}$), in which a lower increase in the accuracy was noticed for the three models ($91.8 \pm 4\%$ for SVM and SLFNN and $92.3 \pm 2\%$ for KNN). When trained on $\tilde{\mathcal{D}}^{f5}$, SLFNN and SVM performed similarly and achieved the highest accuracies of ($96.5 \pm 2\%$) and ($96.2 \pm 6\%$), respectively. Similarly, KNN achieved a satisfactory accuracy ($94.6 \pm 1\%$) when trained on the same dataset, however with a lower standard deviation. It is important to note that KNN and SVM have outperformed the SLFNN algorithm over the four datasets in terms of the standard deviation thus showing a stable performance over the fivefolds and generalization. As a result, SVM outperforms SLFNN and KNN for all the datasets, in which it exhibits the highest discrimination accuracy ($96.5 \pm 2\%$) and low standard deviation when trained on dataset $\tilde{\mathcal{D}}^{f5}$, which contains the features extracted from the whole dataset ($\tilde{\mathcal{D}}$), i.e, varying IS and TL. For that reason, the SVM algorithm was used to demonstrate the impact of varying IS and TL on its discrimination behavior. Fig. 3 illustrates

discrimination behavior of the SVM algorithms when trained on $\tilde{\mathcal{D}}_c^{f2}$ and $\tilde{\mathcal{D}}_c^{f5}$ datasets.

This letter demonstrates the capability of the tactile sensing system to discriminate five different levels of object hardness using feature extraction and ML algorithms. Similar to the work done in [19], the proposed discrimination approach achieves an optimal discrimination accuracy of $\sim 100\%$ when trained on one of the datasets characterized by fixed IS and TL ($\tilde{\mathcal{D}}_c^{f2}$) and the response of a single sensor. Moreover, the proposed approach achieved an accuracy of $96.5 \pm 2\%$ using only five features extracted from the response of a single sensor (16 sensors in [19]) and at variable IS and TL. The SVM algorithm trained on the dataset $\tilde{\mathcal{D}}^{f5}$ achieved an accuracy higher than that in [21] using the same algorithm. Compared to the discrimination approaches presented in [12] and [21], the proposed approach employed PCA to rank the extracted features instead of using it to extract features and train the ML algorithm. This results in a satisfactory accuracy using only two features from a single sensor, thus reducing the complexity of the proposed approach. So far, the available approaches have not considered speed and load as key features for the discrimination problem. However, the current study proved that varying these parameters influences the discrimination behavior of the proposed sensing system. Another important aspect offered by the proposed approach is the scalability, in which its complexity remains acceptable when the system is scaled up in terms of input matrix size and number of classes. In terms of generalization, the proposed approach can be applied to solve new problems (e.g., texture) by fine-tuning or retraining the ML algorithms with new data. Thus, the system must be validated in more active scenarios where daily-life objects are grasped at random loads and speeds.

IV. CONCLUSION

This letter presents a tactile sensing system combined with ML algorithms for hardness discrimination. The system is based on PVDF sensors integrated into a silicon finger cap and embedded electronics. The system was used to collect a dataset representing the system response to indentation stimuli at a variable indentation speed and load. A set of statistical features was extracted from tactile signals and ranked using the PCA biplot for dimension reduction. The features were used to train three classification algorithms (SVM, SLFNN, and KNN). The best discrimination accuracy is ($96.5 \pm 2\%$), which can be obtained using the SVM classifier and five features extracted from a single sensor. Results proved that the performance of the proposed system surpassed the existing hardness discrimination approach. Moreover, this study demonstrated the capability of the proposed system to discriminate the object's hardness while varying the indentation speed and load. The developed approach is robust and suitable for being evaluated in real-time hardness discrimination, for example, sensory restoration in prosthetics or as a high-fidelity sensing system for robotic systems.

ACKNOWLEDGMENT

This work was supported by the AI-Powered Manipulation System for Advanced Robotic Service, Manufacturing and Prosthetics (IntelliMan) project: EU H2022, under Grant 101070136.

REFERENCES

[1] J. Dargahi et al., "Human tactile perception as a standard for artificial tactile sensing - a review," *Int. J. Med. Robot. Comput. Assist. Surg.*, vol. 1, no. 1, 2004, Art. no. 23.
[2] K. Suwanratchatamanee, M. Matsumoto, and S. Hashimoto, "Robotic tactile sensor system and applications," *IEEE Trans. Ind. Electron.*, vol. 57, no. 3, pp. 1074–1087, Mar. 2010.
[3] J. Qu et al., "Recent progress in advanced tactile sensing technologies for soft grippers," *Adv. Funct. Mater.*, vol. 33, no. 41, pp. 1–32, Oct. 2023.
[4] S. Sundaram, "How to improve robotic touch," *Science*, vol. 370, no. 6518, pp. 768–769, Nov. 2020.
[5] H. Liu et al., "Embodied tactile perception and learning," *Brain Sci. Adv.*, vol. 6, no. 2, pp. 132–158, Jun. 2020.
[6] B. Shih et al., "Electronic skins and machine learning for intelligent soft robots," *Sci. Robot.*, vol. 5, no. 41, Apr. 2020, Art. no. 9239.
[7] C. Wang et al., "Tactile sensing technology in bionic skin: A review," *Biosensors Bioelectron.*, vol. 220, 2021, Jan. 2023, Art. no. 114882.
[8] Y. Tang et al., "Optical micro/nanofiber-enabled compact tactile sensor for hardness discrimination," *ACS Appl. Mater. Interfaces*, vol. 13, no. 3, pp. 4560–4566, Jan. 2021.
[9] Y. Tian et al., "Development of flexible tactile sensing arrays for hardness recognition," *Sensors Actuators A: Phys.*, vol. 359, 2023, Art. no. 114478.
[10] Y. Xin et al., "A bionic piezoelectric tactile sensor for features recognition of object surface based on machine learning," *Rev. Sci. Instruments*, vol. 92, no. 9, 2021. [Online]. Available: https://pubs.aip.org/aip/rsi/article/92/9/095003/1032227r
[11] S. Gao, Q. Wang, and L. Yu, "Object recognition based on hardness and texture via modified force-sensitive fingertips of a humanoid hand," *IEEE Sens. Lett.*, vol. 7, no. 2, 2023, Art no. 6000704.
[12] Z. Zhang et al., "Hardness recognition of fruits and vegetables based on tactile array information of manipulator," *Comput. Electron. Agriculture*, vol. 181, 2021, Art. no. 105959.
[13] L. Seminara et al., "Active haptic perception in robots: A review," *Front. Neurorobot.*, vol. 13, pp. 1–20, Jul. 2019.
[14] M. O. Ernst, "Learning to integrate arbitrary signals from vision and touch," *J. Vis.*, vol. 7, no. 5, Jun. 2007, Art. no. 7.
[15] R. S. Johansson et al., "Coding and use of tactile signals from the fingertips in object manipulation tasks," *Nature Rev. Neurosci.*, vol. 10, no. 5, pp. 345–359, 2009.
[16] Y. Pang et al., "Skin-inspired textile-based tactile sensors enable multifunctional sensing of wearables and soft robots," *Nano Energy*, vol. 96, 2022, Art. no. 107137.
[17] H. Fares et al., "Validation of screen-printed electronic skin based on piezoelectric polymer sensors," *Sensors*, vol. 20, no. 4, Feb. 2020, Art. no. 1160.
[18] Y. Abbass et al., "Embedded electrotactile feedback system for hand prostheses using matrix electrode and electronic skin," *IEEE Trans. Biomed. Circuits Syst.*, vol. 15, no. 5, pp. 912–925, Oct. 2021.
[19] Y. Amin et al., "Embedded real-time objects' hardness classification for robotic grippers," *Future Gener. Comput. Syst.*, vol. 148, pp. 211–224, Nov. 2023.
[20] H. Abdi et al., "Principal component analysis," *WIREs Comput. Statist.*, vol. 2, no. 4, pp. 433–459, Jul. 2010.
[21] E. Kerr et al., "Material recognition using tactile sensing," *Expert Syst. Appl.*, vol. 94, pp. 94–111, Mar. 2018.
[22] K. Murakami et al., "A decision method for placement of tactile elements on a sensor glove for the recognition of grasp types," *IEEE/ASME Trans. Mechatron.*, vol. 15, no. 1, pp. 157–162, Feb. 2010.